Supporting Information

Controlling the intersystem crossing/reverse intersystem crossing (ISC/RISC) competition for fulfilling efficient red metal-free phosphorescent molecules.

Daokun Zhong, Ruiqin Zhu, Zhao Feng, Jie Zhang, Bochao Su, Yuanhui Sun, Xiaolong Yang*, Ling Yue*, Guijiang Zhou*

School of Chemistry, Engineering Research Center of Energy Storage Materials and Devices, Ministry of Education, Xi'an Key Laboratory of Sustainable Energy Materials Chemistry, Xi'an Jiaotong University, Xi'an 710049, China.

*Corresponding Author(s):

Xiaolong Yang：xiaolongyang@xjtu.edu.cn

Ling Yue：heartstar@mail.xjtu.edu.cn

Guijiang Zhou：zhougj@mail.xjtu.edu.cn

Table of Contents

1 Experimental Procedures

1.1 General Information. Commercial chemicals were used without further purification. All reactions were carried out under nitrogen atmosphere. Prior to use, solvents were carefully dried and distilled from appropriate drying agents. All reactions were monitored by thin-layer chromatography (TLC) from Merck & Co., Inc. Column chromatography and preparative TLC was conducted by using silica gel from Shanghai Qingdao (300-400 mesh). ^{1}H, and ^{13}C NMR spectra were recorded in CDCl3 on a Bruker Avance 400 or 600 MHz spectrometer. The chemical shifts were quoted on the solvent residual peak at δ 7.26 ppm for ^{1}H and 77.0 ppm for ^{13}C, respectively. Mass spectra (MS) were recorded on a WATERS I-Class VION IMS Qtof mass spectroscopy. The thermal gravimetric analysis (TGA) was tested with a NETZSCH STA 409C instrument under N_2 at a heating rate of 20 K min^{-1}. UV-vis spectra were recorded on a Shimadzu UV-2250 spectrophotometer. The photoluminescent spectra and lifetimes were measured on Edinburgh Instruments FLS920 spectrophotometer. The photoluminescent quantum yields (PLQYs) were determined in CH_2Cl_2 solutions with an integrating sphere. With a scan rate of 100

mV s^{-1}, cyclic voltammetry measurements were carried out on a Princeton Applied Research model 2273A potentiostat through three-electrode configuration with a glassy carbon working electrode, a Pt-sheet counter electrode and a Pt-wire reference electrode in electrolyte of 0.1 M $[Bu_4N]PF_6$ in degassed CH_3CN. The femtosecond transient absorption spectra and The nanosecond transient absorption spectra were tested with a PH_2 Laser System by LIGHT CONVERSION and measured in neat films under 380 nm excitation.

1.2 Theoretical investigation. Geometry optimization and vertical excitation energy calculations PhODCB, PhSDCB and PhSeDCB have been carried out by means of Density function theory (DFT) and time-dependent density functional theory (TD-DFT) as implemented in the Gaussian 09[1] package. Spin-orbit coupling was studied in the Dalton 2016[2] package under the same functional/basis set in vacuum based on the ground state geometry optimized in Gaussian 09. Preliminary TD-DFT calculations have been performed to set up the methodology to be used; the calculated UV-vis spectra of PhODCB, PhSDCB and PhSeDCB in TOL using various functionals and basis sets are compared with their experimental spectra. Experimental spectra could be well reproduced at the e B3LYP/6-311G** level[3,4] level.

1.3 Synthesis.

The key intermediate compound PhCB was synthesized according the literature methods[5] with the synthetic details and steps (Shamed S1) presented in Supporting Information (SI). The key intermediate compounds PhODI, PhSDI and PhSeDI were synthesized with the synthetic details and steps (Shamed S1) presented in SI. The synthetic strategies for the target compounds of

PhODCB, PhSDCB and PhSeDCB were outlined in Scheme 1.

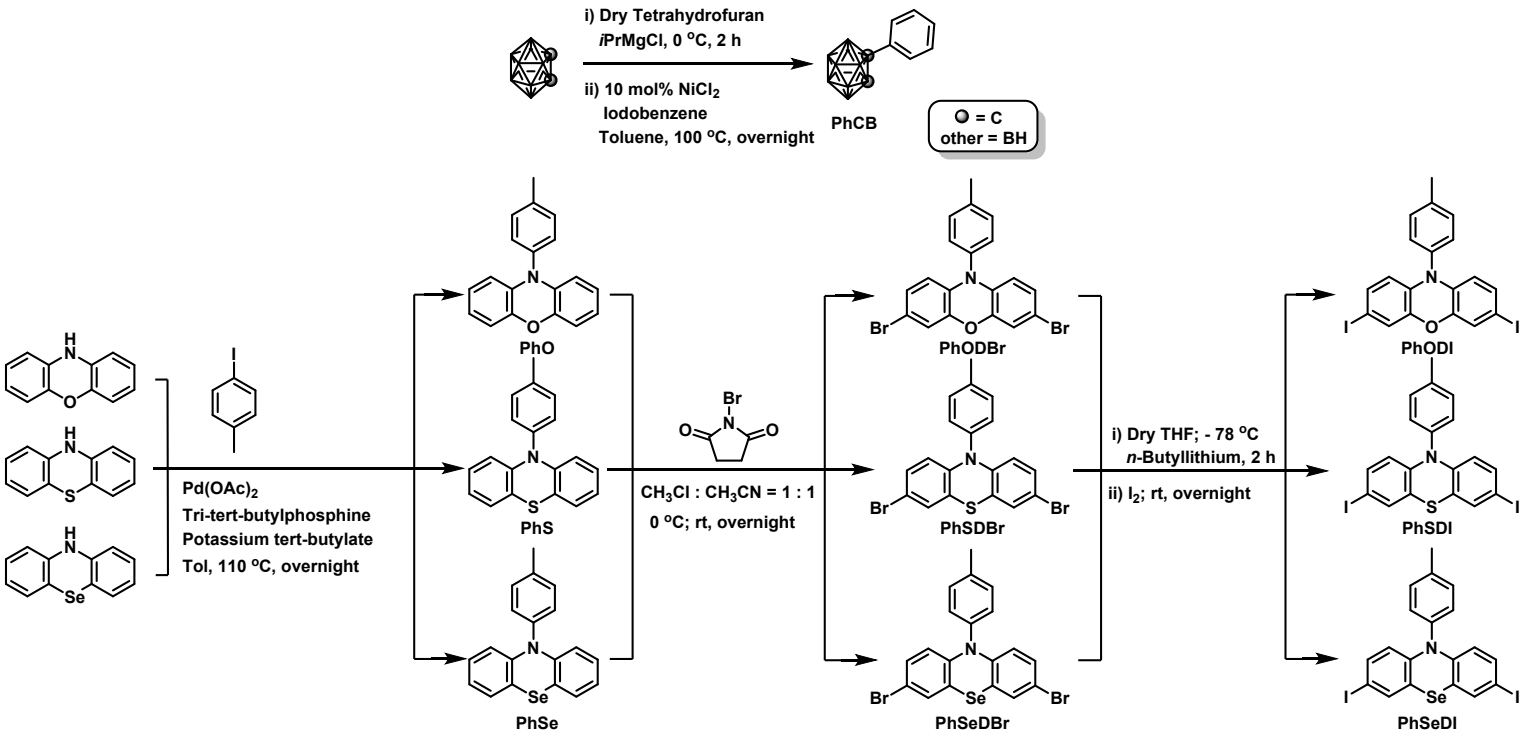

Shamed S1. Synthesis of the key intermediate compounds .

Synthesis of PhCB. iPrMgCl (2.0 m in THF, 1.31 mL, 2.62 mmol) was slowly added to a THF solution (10 mL) of o-carborane (288 mg, 2.18 mmol) at 0 °C, and the mixture was stirred at 0 °C for 2 h. After replacement of THF with toluene (5 mL), and addition of iodobenzene (534 mg, 2.62 mmol) and $NiCl_2$ (5.2 mg, 0.04 mmol), the reaction mixture was heated at 100 °C under stirring for 12 h in a closed flask. Then, the reaction was quenched with water (10 mL) and extracted with diethyl ether. The ether solutions was combined and concentrated to dryness in vacuo. The residue was subjected to flash column chromatography on silica gel (300–400 mesh) using petroleum ether as eluent to give PhCB. Yield: 94%. ^{1}H NMR (400 MHz, CDCl3) 7.49 (d, *J* = 7.3 Hz, 2 H), 7.39 (d, *J* = 7.1 Hz, 1H), 7.34 (d, *J* = 7.8 Hz, 2 H), 3.31–1.54 (m, 10 H).

General Procedure for Synthesis of PhO, PhS and PhSe. Under nitrogen atmosphere, methyl 5-bromo-2-iodobenzoate (1.2 equivalent), the corresponding donor compound (1.0 equiv),

Pd(OAc)2 (0.06 equivalent), tri-ter-butylphosphine (0.06 equiv) and Sodium ter-butoxide (4 equiv) was added to a Schlenk tube containing toluene. The resulting mixture was stirred at 110 °C for 18 h. After cooling to room temperature, the mixture was filtered, the organic phase was washed with water and extracted into dichloromethane, then dried with anhydrous Na_2SO_4, evaporated to dryness. The residue was subjected to flash column chromatography on silica gel (300–400 mesh) using petroleum ether as eluent to give PhO, PhS and PhSe.

PhO: Yield: 82%. ^{1}H NMR (400 MHz, $CDCl_3$): 7.39 (d, *J* = 8.0 Hz, 2 H), 7.21 (d, *J* = 8.2 Hz, 2 H), 6.76 – 6.45 (m, 6 H), 5.92 (d, *J* = 7.7 Hz, 2 H), 2.45 (s, 3 H).

PhS: Yield: 78%. ^{1}H NMR (400 MHz, $CDCl_3$): 7.44 – 7.37 (m, 2 H), 7.27 (d, *J* = 7.1 Hz, 2 H), 7.06 – 6.93 (m, 2 H), 6.75 (dd, *J* = 8.8, 1.0 Hz, 2 H), 6.19 (dd, *J* = 8.8, 1.2 Hz, 2 H), 2.47 (s, 3 H).

PhSe: Yield: 70%. ^{1}H NMR (400 MHz, $CDCl_3$) δ 7.35 (d, *J* = 8.4 Hz, 2 H), 7.28 – 7.21 (m, 4 H), 6.97 – 6.92 (m, 2 H), 6.85 (td, *J* = 7.6, 1.2 Hz, 2 H), 6.51 (dd, *J* = 8.4, 1.2 Hz, 2 H), 2.44 (s, 3 H).

General Procedure for Synthesis of PhODBr, PhSDBr and PhSeDBr. A solution of PhO, PhS and PhSe (1.0 equiv) in CH_3Cl : CH_3CN = 1 : 1 (V : V) was added dropwise into the solution of NBS (2.2 equiv) and stirred 30 min at 0 °C, then the mixture was stirred overnight at room temperature. After the reaction was completed, the reaction was quenched with sodium thiosulfate solution and extracted with dichloromethane. The organic layer dried with anhydrous Na_2SO_4, evaporated to dryness. The residue was subjected to flash column chromatography on silica gel (300–400 mesh) using petroleum ether as eluent to give PhODBr, PhSDBr and PhSeDBr.

PhODBr: Yield: 84%. ^{1}H NMR (400 MHz, $CDCl_3$): 7.38 (d, *J* = 8.1 Hz, 2 H), 7.15 (d, *J* = 8.2 Hz, 2H), 6.79 (d, *J* = 2.2 Hz, 2 H), 6.68 (dd, *J* = 8.5, 2.2 Hz, 2 H), 5.76 (d, *J* = 8.5 Hz, 2 H), 2.44 (s, 3H).

PhSDBr: Yield: 76%. ^{1}H NMR (400 MHz, $CDCl_3$): 7.47–7.33 (m, 2 H), 7.20 (d, *J* = 7.9 Hz, 2 H), 7.06 (d, *J* = 10.8 Hz, 2 H), 6.93–6.84 (m, 2 H), 2.46 (s, 3 H).

PhSeDBr: Yield: 69%. ^{1}H NMR (400 MHz, $CDCl_3$) δ 7.42 (d, *J* = 8.4 Hz, 2 H), 7.23 – 7.20 (m, 2 H), 6.95 – 6.90 (m, 2 H), 6.82 (td, *J* = 7.6, 1.2 Hz, 2 H), 6.53 (dd, *J* = 8.4, 1.2 Hz, 2 H), 2.45 (s, 3 H).

General Procedure for Synthesis of PhODI, PhSDI and PhSeDI. Under nitrogen atmosphere, A solution of PhODBr, PhSDBr and PhSeDBr (1.0 equiv) in dry THF was cooled to – 78 °C. Then, n-BuLi (2.1 equiv) was added dropwise and stirred 90 min at this temperature. After that, I_2 (2.1 equiv) was added. The reactive mixture was warmed to room temperature and stirred for 3 h. The reaction was quenched with 5% sodium thiosulfate solution. The reaction mixture was extracted with dichloromethane and dried with anhydrous Na_2SO_4. The residue was subjected to flash column chromatography on silica gel (300–400 mesh) using petroleum ether as eluent to give the mimixture with PhODI, PhSDI, PhSeDI and their side products of debromination. Due to the inability to purify, proceed directly to the next reaction step.

General Procedure for Synthesis of PhODCB, PhSDCB and PhSeDCB. iPrMgCl (2.0 m in THF, 2.2 equiv) was slowly added to a THF solution of o-carborane (2.1 equiv) at 0 °C, and the mixture was stirred at 0 °C for 2 h. After replacement of THF with toluene, and addition of aryl iodide (1.0 equiv) and $NiCl_2$ (0.04 equiv), the reaction mixture was heated at 100 °C under stirring for 12 h in a closed flask. Then, the reaction was quenched with water and extracted with diethyl ether. The ether solutions were combined and concentrated to dryness in vacuo. The residue was subjected to flash column chromatography on silica gel (300–400 mesh) using petroleum ether / ethyl acetate (20:1, v /v) as eluent to give PhODCB, PhSDCB and PhSeDCB.

PhODCB: Yield: 73%. ^{1}H NMR (400 MHz, $CDCl_3$): 7.44 (d, J = 8.3 Hz, 4 H), 7.30 (t, J = 8.0 Hz, 4 H), 7.21 (t, J = 7.6 Hz, 4 H), 6.95 (d, J = 8.1 Hz, 2 H), 6.66 (s, 2 H), 6.59 (dd, J = 8.6, 1.9 Hz, 2 H), 5.56 (d, J = 8.6 Hz, 2 H), 3.72 – 1.71 (m, 20 H), 2.39 (s, 3 H). ^{13}C NMR (151 MHz, $CDCl_3$): 142.73, 139.34, 135.08, 134.14, 131.85, 130.78, 130.71, 130.23, 129.50, 128.42, 126.38, 124.28, 117.59, 112.57, 85.51, 85.02, 21.23. ESI-MS (m/z): theoretical $[M-e]^+$ 713.52003, found: 713.52353.

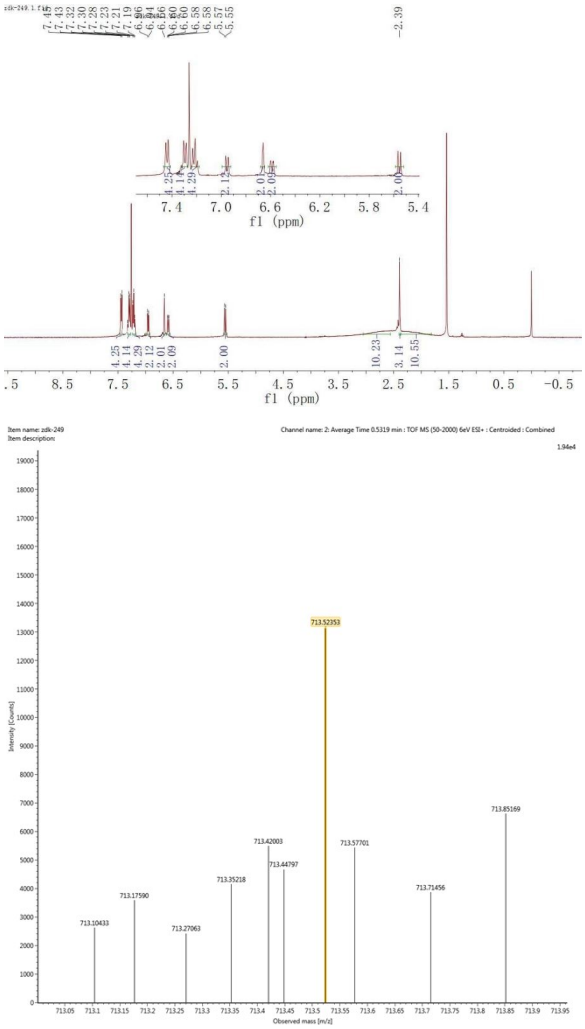

PhSDCB: Yield: 69%. ^{1}H NMR (400 MHz, $CDCl_3$):7.42 (d, J = 7.9 Hz, 4 H), 7.31 (d, J = 8.1 Hz, 4 H), 7.20 (t, J = 7.6 Hz, 4 H), 6.99 (d, J = 8.1 Hz, 2 H), 6.87 (s, 2H), 6.77 (dd, J = 8.9, 2.1 Hz, 2 H), 5.72 (d, J = 8.8 Hz, 2 H), 3.72 – 1.81 (m, 20 H), 2.41 (s, 3 H). ^{13}C NMR (151 MHz, $CDCl_3$): 144.57, 139.20, 136.43, 131.75, 130.70, 130.66, 130.27, 130.04, 129.51, 128.44, 128.25, 125.33,

118.46, 114.82, 85.40, 84.56, 21.22. ESI-MS (m/z): theoretical $[M+K]^+$ 768.44089, found: 768.44214.

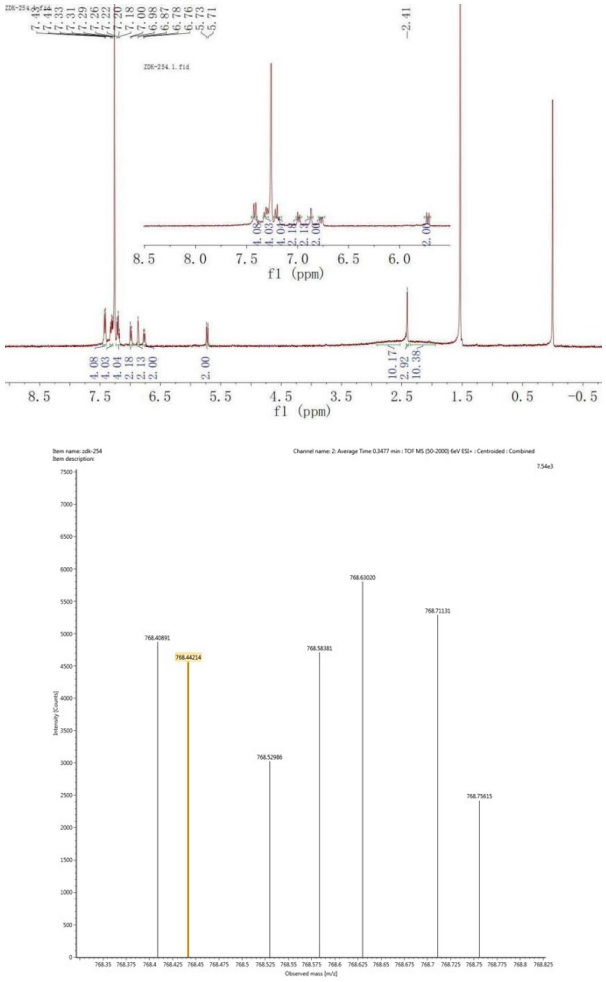

PhSeDCB: Yield: 65%. ^{1}H NMR (400 MHz, $CDCl_3$): 7.42 (d, J = 7.8 Hz, 4 H), 7.30 (t, J = 7.3 Hz, 4 H), 7.19 (t, J = 7.5 Hz, 4H), 7.07 (s, 2 H), 7.01 (d, J = 7.9 Hz, 2 H), 6.84 (d, J = 8.8 Hz, 2 H), 5.90 (d, J = 8.8 Hz, 2 H), 3.72 – 1.65 (m, 20 H), 2.41 (s, 3 H). ^{13}C NMR (151 MHz, $CDCl_3$): 145.04, 139.04, 137.48, 131.57, 130.95, 130.71, 130.69, 130.28, 129.77, 128.45, 125.77, 116.09, 113.96, 85.44, 84.55, 21.23. ESI-MS (m/z): theoretical $[M+Li]^+$ 784.45764, found: 784.45881.

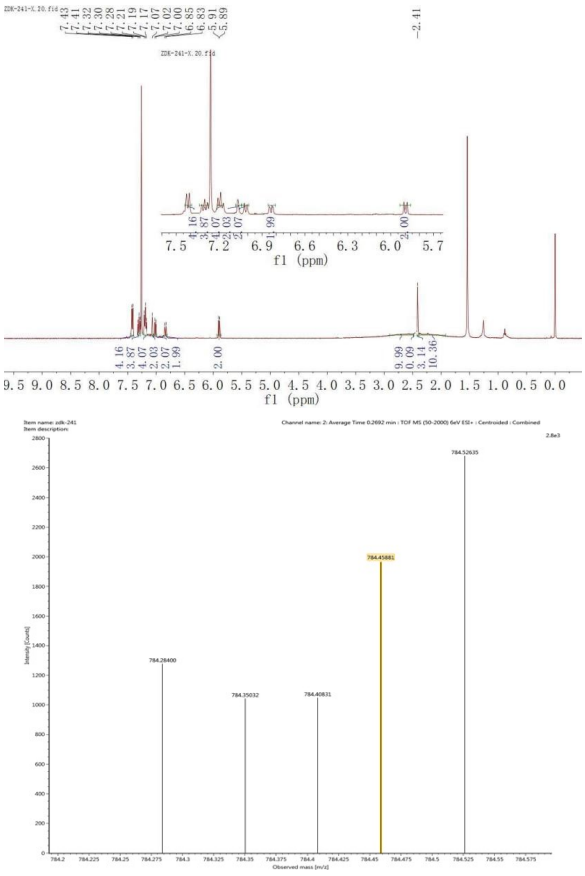

2 Results and Discussion

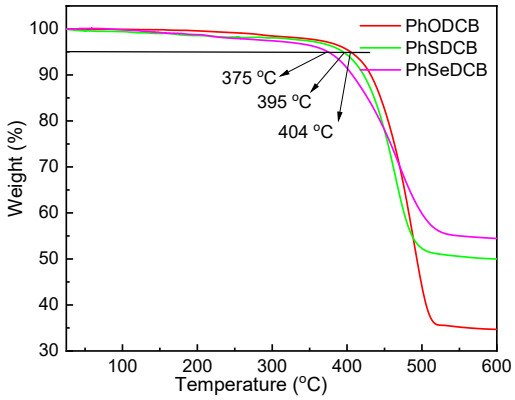

Figure S1. TGA curves of PhODCB, PhSDCB and PhSeDCB.

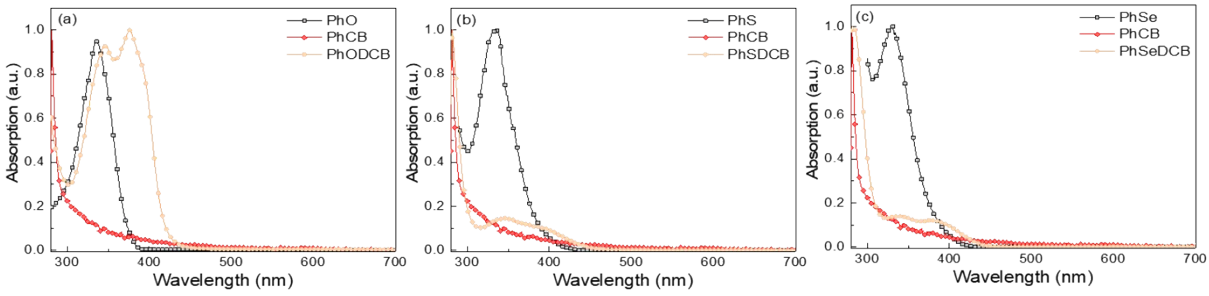

Figure S2. UV-vis absorption spectra of (a) PhO, PhCB, PhODCB; (b) PhS, PhCB, PhSDCB and

(c) PhSe, PhCB, PhSeDCB in toluene solutions.

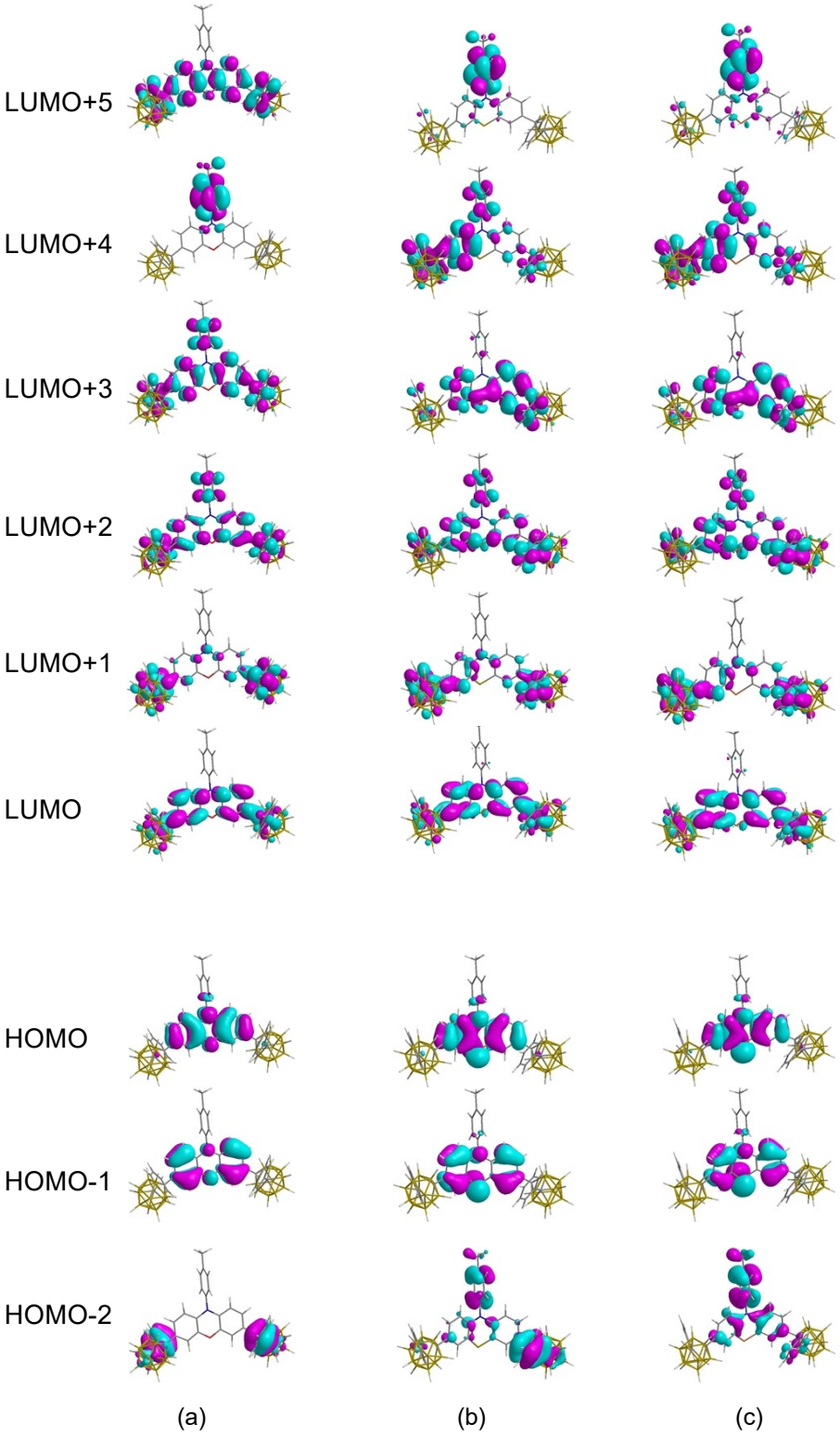

Figure S3. Molecular orbital patterns (isocontour value = 0.025) for (a) PhODCB, (b) PhSDCB and (c) PhSeDCB based on their optimized S_0 geometries.

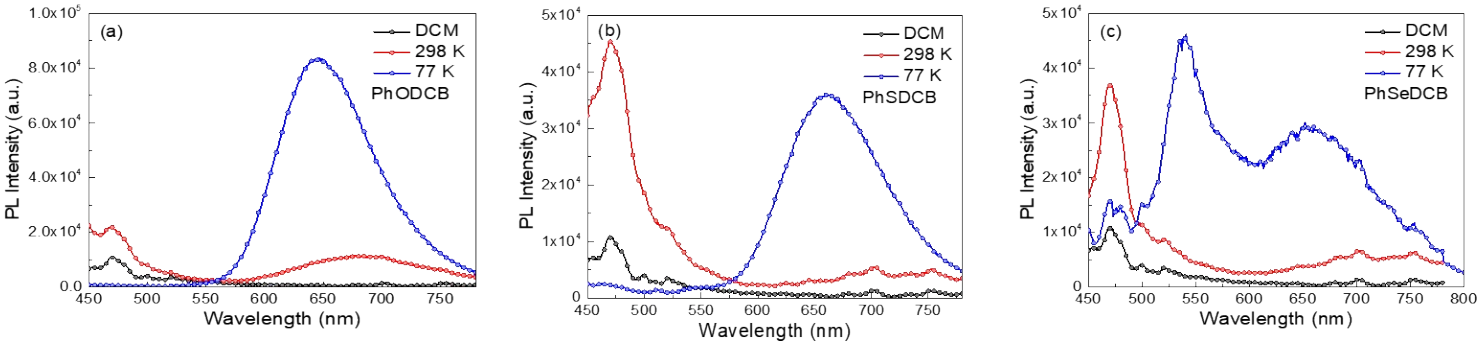

Figure S4. PL spectra of PhODCB, PhSDCB, and PhSeDCB in dichloromethane solution at 298 K.

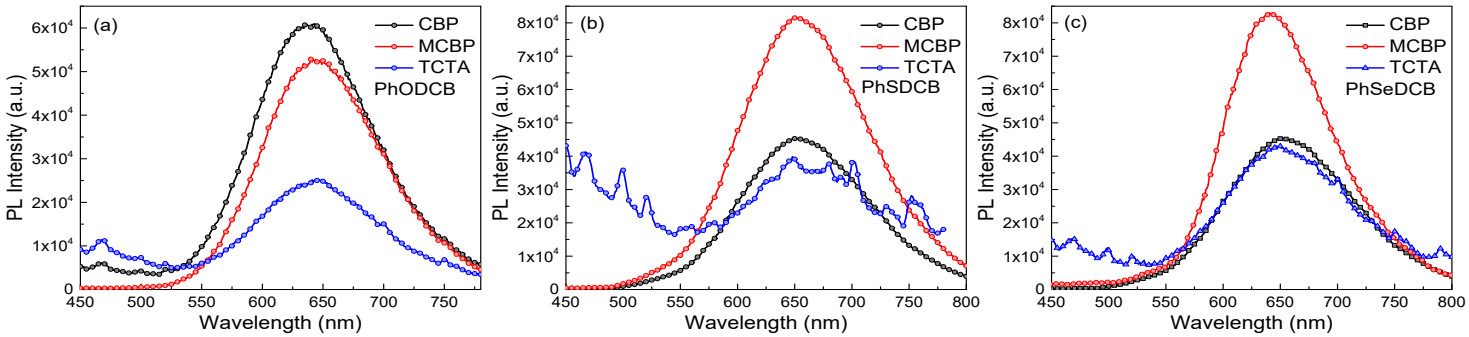

Figure S5. PL spectra of PhODCB, PhSDCB, and PhSeDCB doped in CBP, mCBP and TCTA at 298 K.

Table S1. PL Data of PhODCB, PhSDCB and PhSeDCB in different host.

	Host	Emission λem (nm)	PLQY[a]
PhODCB	CBP	640	46.4%
	mCBP	644	30.4%
	TCTA	644	18.4%
PhSDCB	CBP	650	34.3%
	mCBP	654	30.4%
	TCTA	654	9.2%
PhSeDCB	CBP	646	23.6%
	mCBP	653	48.3%
	TCTA	653	9.5%

[a]Absolute photoluminescent quantum yields (PLQY).

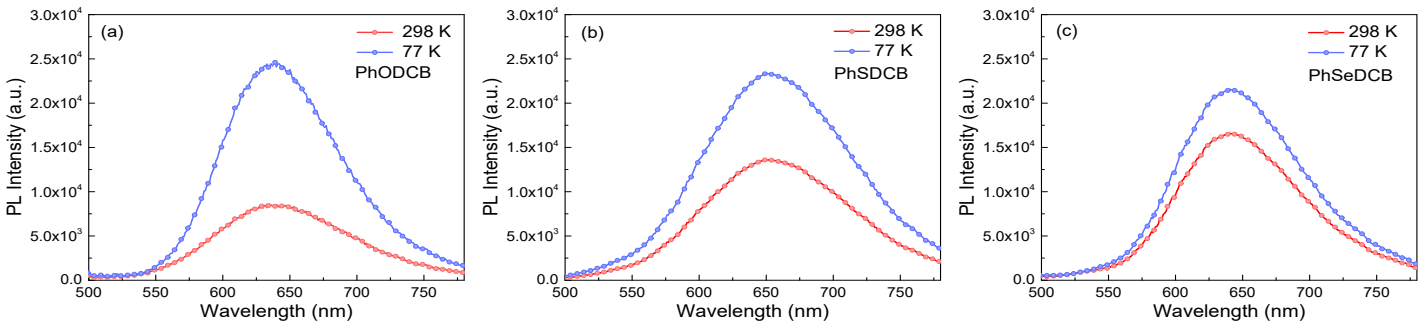

Figure S6. PL spectra at both 298 K and 77 K of PhODCB, PhSDCB and PhSeDCB in the mCBP films.

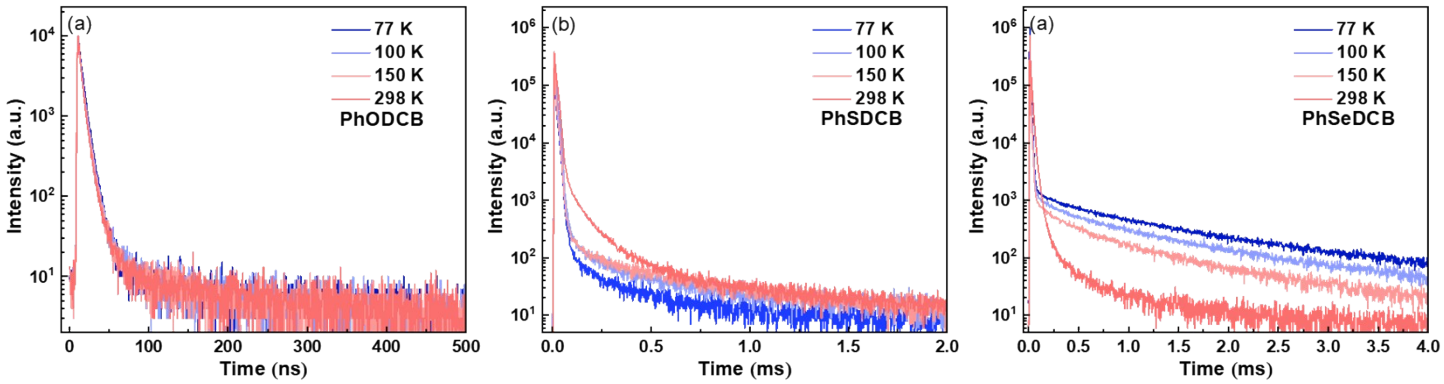

Figure S7. The transient PL decay data under nitrogen for these three emitters measured in non-doped films.

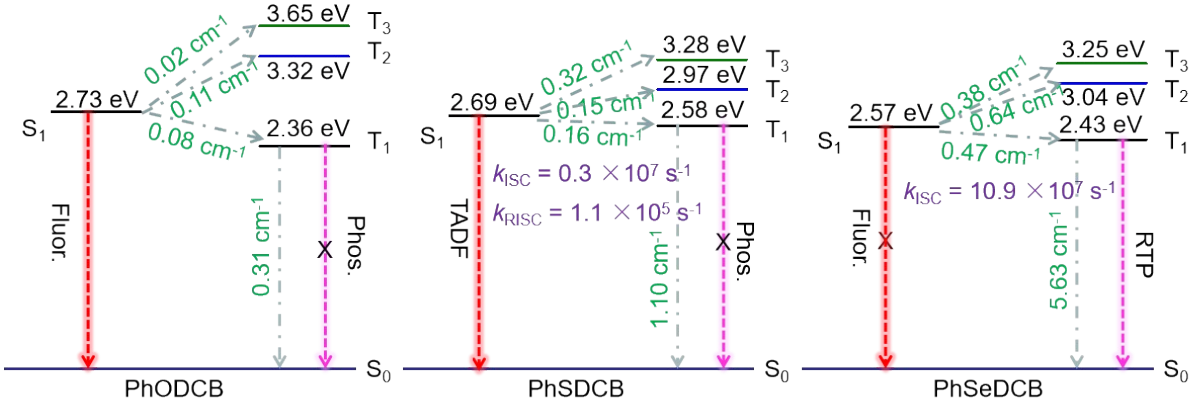

Figure S8. Spin−orbit coupling matrix elements (SOCMEs) for PhODCB, PhSDCB and PhSeDCB with energetic levels of S_1 excited states. SOC elements are calculated from $\sqrt{\sum\langle S_n|\hat{H}_{SO}|^2 T_{n,M_s=0,\pm1}\rangle}$.

Table S2. Summary of the exciton energy level and dynamic rate constants of the investigated compounds in 5 wt.% mCBP doped films

Compound	S_1 (eV)	T_1 (eV)	ΔE_{ST} (eV)	Φ_P [a] (%)	Φ_{PF} [b]	Φ_{DF} [c] (%)	τ_{PF} [d] (ns)	τ_{DF} [e] (μs)	τ_P [f] (μs)	k_{PF} (10^6 s^{-1})	k_{DF} (10^4 s^{-1})	k_{ISC} (10^7 s^{-1})	k_{RISC} (10^5 s^{-1})

					(%)								
PhODCB	2.73	2.36	0.37		30.4	--	9.5	--	--	--	--	--	--
PhSDCB	2.69	2.58	0.11		4.0	26.4	12.3	17.5	--	3.3	1.5	0.3	1.1
PhSeDCB	2.57	2.43	0.14	48.3	--	--	9.2	--	14.7	--	--	10.9	--

[a] Phosphorescence Quantum Yield, [b]The prompt fluorescence quantum yields, c delayed fluorescence quantum yields, [d]The prompt fluorescence lifetime, [e]delayed fluorescence lifetime, [f]The phosphorescence lifetime. The experimental data of S_1 was determined from onsets of the absorption spectrum (298 K). The experimental data of T_1 was determined from onsets of the phosphorescence (77 K) spectra. The rate constants of PF and DF (k_{PF} and k_{DF}) evalvuated according to experimental data: $k_{PF} = \Phi_{PF} / \tau_{PF}$ and $k_{DF} = \Phi_{DF} / \tau_{DF}$ for PhSDCB. Φ_{DF} is the absolute quantum yield measured under μs-level pulsed light at 100 Hz. The rate constants of intersystem crossing and reverse (k_{ISC} and k_{RISC}) are further estimated according to $k_{ISC} = \Phi_{DF}\, k_{PF} / (\Phi_{PF} + \Phi_{DF})$ and $k_{RISC} = k_{DF}\, k_{PF}\, \Phi_{DF} / (k_{ISC}\, \Phi_{PF})$ for PhSDCB. Because of the dominated phosphorescence emission with neglect fluorescence and high phosphorescence quantum yields, we assume that the radiative and non-radiative transition of singlet can be ignored, thus the prompt lifetime (τ_{PF}) for PhSeDCB is 9.2 ns (Figur S7), thus, the k_{ISC} in the film state is calculated as $k_{ISC} = 1 / \tau_{PF}$.

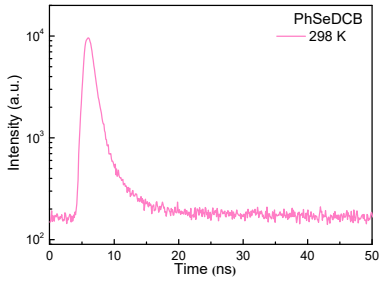

Figure S9. Transient PL decay spectra of PhSeDCB in 5 wt.% mCBP doped films.

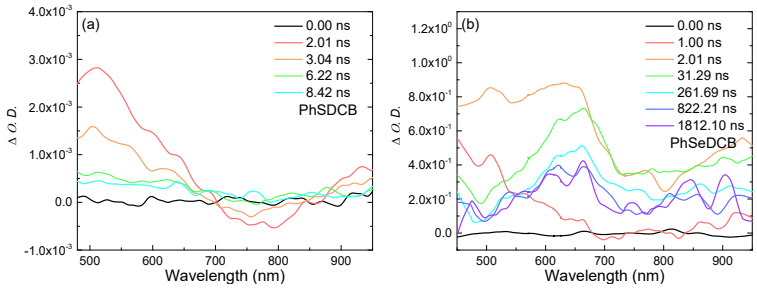

Figure S10. The nanosecond transient absorption spectra were measured in neat films under 380 nm excitation of PhSDCB and PhSeDCB.

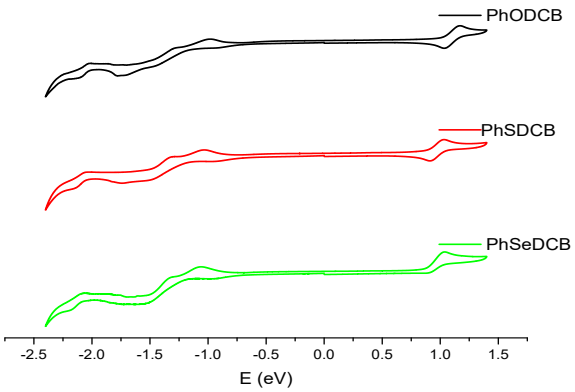

Figure S11. Cyclic curves of PhODCB, PhSDCB and PhSeDCB measured in CH_3CN at room temperature.

Table S3. Redox Properties of PhODCB, PhSDCB and PhSeDCB

Compound	E_{pa} (V)	E_{pc} (V)	E_{HOMO} (eV) [c]	E_{LUMO} (eV)[d]	E_g^{CV} (eV)[e]
PhODCB	0.69a	-1.24b	-5.49	-3.56	1.93
PhSDCB	0.51a	-1.30 b	-5.31	-3.50	1.81
PhSeDCB	0.50a	-1.25 b	-5.30	-3.55	1.75

[a] Reversible. The value was set as $E_{1/2}$. [b] Irreversible. The value was derived from the cathodic peak potential. [c] E_{HOMO} = – (4.8 + E_{pa}) eV. [d] E_{LUMO} = – (4.8 + E_{pc}) eV, E_{pc} : First reduction potential. [e] CV energy gap E_g^{cv} = LUMO – HOMO.

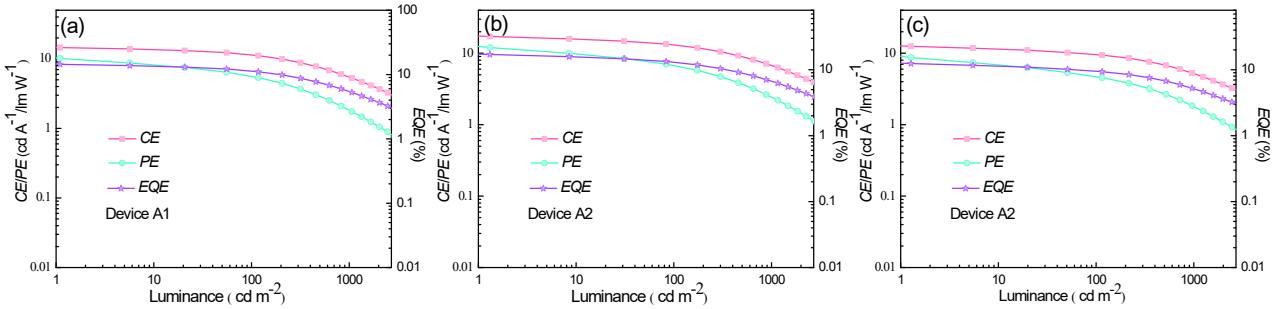

Figure S12. Relationship between EL efficiencies and luminance for the devices. (a) Device A1, (b) Device A2 and (c) Device A3.

Table S4. EL Performance of PhSeDCB based devices.

Device	Dopant	$V_{turn-on}$ (V)	Luminance L_{max} (cd m^{-2}) [a]	EQE (%)	CE (cd A^{-1})	PE (lm W^{-1})	λ_{max} (nm) [d]
A1	PhSeDCB (2.0 wt %)	2.5	4419.6 (15.0)	14.9 (3.5) [a]	15.0 (3.5)	17.9 (2.5)	676
				11.1 [b]	11.2	5.4	(0.61, 0.34)
				5.3 [c]	5.3	1.8	
A2	PhSeDCB (3.0 wt %)	2.5	5962.7 (15.0)	18.6 (3.5) [a]	18.7 (3.5)	22.0 (2.5)	676
				13.4 [b]	13.4	6.8	(0.61, 0.34)
				7.0 [c]	6.4	2.3	
A3	PhSeDCB(4.0wt %)	2.5	5155.2 (14.0)	13.9 (3.0) [a]	14.0 (3.0)	17.1 (2.5)	676
				9.3 [b]	9.5	4.6	(0.61, 0.34)
				5.2 [c]	5.3	1.6	

[a] Maximal values of these devices. Values in the parentheses are the voltages at which they were obtained. [b] Values collected at 100 cd m^{-2}. [c] Values collected at 1000 cd m^{-2}. [d] Values are collected at 10 V for devices A1-A3 and CIE coordinates (x, y) are shown in parentheses.

Table S5. PL and EL performances of the representative systems for RTP emitters.

RTP emitters	λ_{EL} (nm)	PLQY (%)	τ_P (ms)	EL			Ref.
				CE (cdA^{-1})	PE ($lm\ W^{-1}$)	EQE (%)	
PhSeDCB	676	48.3	0.01	18.7	22.0	18.6	This work
PhSeDB	532	77.8	0.63	53.6	49.6	18.2	[6]
PhSeB	512	67.0	0.65	29.5	24.1	10.5	[6]
PhSe	497	28.8	0.84	24.1	17.3	7.5	[7]
mPhSe	498	33.9	0.44	27.5	21.6	8.7	[7]
BuPhSe	496	34.0	0.44	28.4	22.3	9.0	[7]
PSe1	535	33.0	0.61	–	–	10.7	[8]
PSe2	535	35.0	0.64	–	–	10.0	[8]
PSe3	530	27.0	0.93	–	–	8.1	[8]
PSe3Cz	540	50.2	0.82	45.9	–	13.2	[9]
BPXSeDRZ	564	66.3	2.10	53.7	48.2	17.2	[10]
DBPXSeDRZ	575	66.9	1.70	46.7	40.2	17.9	[10]
3,2-PIC-XT	504	65.0	0.0024	87.9	96.8	30.8	[11]
3,2-PIC-TXT	508	98.0	0.0014	90.2	96.6	33.2	[12]

3 Calculated SOCME between triplets and singlets data.

Table S6. Spin−orbit coupling matrix elements (SOCMEs) data for PhODCB, PhSDCB and PhSeDCB with energetic levels of T_1 excited states.

	Root		<T|HSO|S> (Re, Im) cm^{-1}		
	T	S	Z	X	Y
PhODCB	1	0	(0.00, -0.01)	(0.00, -0.03)	(-0.00, -0.31)
	1	1	(0.00, -0.08)	(0.00, 0.00)	(-0.00, 0.00)
	2	1	(0.00, 0.00)	(0.00, 0.06)	(-0.00, 0.09)
	3	1	(0.00, 0.02)	(0.00, -0.00)	(-0.00, 0.00)
PhSDCB	1	0	(0.00, 0.58)	(0.00, -0.16)	(-0.00, 0.92)
	1	1	(0.00, -0.08)	(0.00, 0.03)	(-0.00, 0.13)
	2	1	(0.00, 0.15)	(0.00, -0.02)	(-0.00, -0.00)
	3	1	(0.00, 0.24)	(0.00, -0.01)	(-0.00, -0.21)
PhSeDCB	1	0	(0.00, -4.06)	(0.00, 0.21)	(-0.00, -3.90)
	1	1	(0.00, -0.30)	(0.00, -0.06)	(-0.00, -0.35)
	2	1	(0.00, -0.44)	(0.00, -0.31)	(-0.00, -0.35)
	3	1	(0.00, -0.27)	(0.00, -0.14)	(-0.00, 0.23)

Table S7. Spin−orbit coupling matrix elements (SOCMEs) data for PhODCB, PhSDCB and PhSeDCB with energetic levels of S_1 excited states.

	Root		<T|HSO|S> (Re, Im) cm^{-1}		
	T	S	Z	X	Y
PhODCB	1	0	(0.00, -0.52)	(0.00, -0.16)	(-0.00, -0.64)
	1	1	(0.00, -0.17)	(0.00, -0.05)	(-0.00, -0.19)
	2	1	(0.00, 0.09)	(0.00, 0.06)	(-0.00, 0.06)
	3	1	(0.00, -0.24)	(0.00, 0.08)	(-0.00, -0.27)
PhSDCB	1	0	(0.00, -0.21)	(0.00, 0.25)	(-0.00, -0.81)
	1	1	(0.00, -0.09)	(0.00, 0.03)	(-0.00, 0.15)
	2	1	(0.00, 0.17)	(0.00, -0.02)	(-0.00, -0.06)
	3	1	(0.00, 0.22)	(0.00, 0.02)	(-0.00, -0.21)
PhSeDCB	1	0	(0.00, 2.83)	(0.00, -0.53)	(-0.00, 3.31)
	1	1	(0.00, -0.29)	(0.00, -0.06)	(-0.00, -0.36)
	2	1	(0.00, -0.40)	(0.00, -0.23)	(-0.00, -0.15)
	3	1	(0.00, -0.15)	(0.00, -0.11)	(-0.00, 0.23)

4 References

1. M. J. Frisch, G. W. T., H. B. Schlegel, G. E. Scuseria, M. A. Robb, J. R. C., G. Scalmani, V. Barone, B. Mennucci, G. A. Petersson, H. N., M. Caricato, X. Li, H. P. Hratchian, A. F. Izmaylov, J. B., G. Zheng, J. L. Sonnenberg, M. Hada, M. Ehara, K. T., R. Fukuda, J. Hasegawa, M. Ishida, T. Nakajima,; Y. Honda, O. K., H. Nakai, T. Vreven, J. A. Montgomery, Jr., J. E. Peralta, F. O., M. Bearpark, J. J. Heyd, E. Brothers, K. N. Kudin, V. N. S., T. Keith, R. Kobayashi, J. Normand, K. Raghavachari, A. R., J. C. Burant, S. S. Iyengar, J. Tomasi, M. Cossi, N. R., J. M. Millam, M. Klene, J. E. Knox, J. B. Cross, V. Bakken, C. A., J. Jaramillo, R. Gomperts, R. E. Stratmann, O. Yazyev, A. J. A., R. Cammi, C. Pomelli, J. W. Ochterski, R. L. Martin, K. M., V. G. Zakrzewski, G. A. Voth, P. Salvador, J. J. D., S. Dapprich, A. D. Daniels, O. Farkas, J. B. F., J. V. Ortiz, J. Cioslowski, Fox, D. J. Gaussian 09, Revision B.01, Gaussian, Inc., Wallingford CT, 2010.

2. Aidas, K., Angeli, C., Bak, K. L., Bakken, V., Bast, R., Boman, L., Christiansen, O., Cimiraglia, R., Coriani, S., Dahle, P., Dalskov, E. K., Ekström, U., Enevoldsen, T., Eriksen, J. J., Ettenhuber, P., Fernández, B., Ferrighi, L., Fliegl, H., Frediani, L., Hald, K., Halkier, A., Hättig, C., Heiberg, H., Helgaker, T., Hennum, A. C., Hettema, H., Hjertenæs, E., Høst, S., Høyvik, I.-M., Iozzi, M. F., Jansík, B., Jensen, H. J. A., Jonsson, D., Jørgensen, P., Kauczor, J., Kirpekar, S., Kjærgaard, T., Klopper, W., Knecht, S., Kobayashi, R., Koch, H., Kongsted, J., Krapp, A., Kristensen, K., Ligabue, A., Lutnæs, O. B., Melo, J. I., Mikkelsen, K. V., Myhre, R. H., Neiss, C., Nielsen, C. B., Norman, P., Olsen, J., Olsen, J. M. H., Osted, A., Packer, M. J., Pawlowski, F., Pedersen, T. B., Provasi, P. F., Reine, S., Rinkevicius, Z., Ruden, T. A., Ruud, K., Rybkin, V. V., Sałek, P., Samson, C. C. M., de Merás, A. S., Saue, T., Sauer, S. P. A., Schimmelpfennig, B., Sneskov, K., Steindal, A. H., Sylvester-Hvid, K. O., Taylor, P. R., Teale, A. M., Tellgren, E. I., Tew, D. P.,

Thorvaldsen, A. J., Thøgersen, L., Vahtras, O., Watson, M. A., Wilson, D. J. D., Ziolkowski, M., Ågren, H., WIREs Comput. Mol. Sci., 2014, 4, 269.
3. Becke, A. D., J. Chem. Phys. 1993, 98, 5648.
4. Stephens, P. J., Devlin, F. J., Chabalowski, C. F., Frisch, M. J., J. Phys. Chem. 1994, 98, 11623.
Tang C, Xie Z., Angew. Chem., 2015, 127: 7772-7775.
D. K. Zhong, S. Q. Liu, L. Yue, F. Zhao, H. Y. Wang, P. Yang, B. C. Su, X. L. Yang, Y. H. Sun, G. J. Zhou, Chem. Scie., 2024, 15: 9112-9119.
7. C. L. Kim, J. Jeong, H. J. Jang, K. H. Lee, S.-T. Kim, M.-H. Baik, J. Y. Lee, J. Mater. Chem. C, 2021, 9, 8233-8238.
8. D. R. Lee, K. H. Lee, W. Shao, C. L. Kim, J. Kim, J. Y. Lee, Chem. Mater., 2020, 32, 2583-2592.
9. C. L. Kim, J.-M. Kim, H. Jang, D. R. Lee, J. Y. Lee, ACS Appl. Energy Mater., 2022, 5, 4985-4990.
10. Z. Chen, Q. Gu, M. Li, W. Qiu, Y. Jiao, X. Peng, W. Xie, D. Liu, K. Liu, Z. Yang, S. J. Su, Adv. Opt. Mater., 2024, 2302503.
11. X. Peng, P. Zou, J. Zeng, X. Wu, D. Xie, Y. Fu, D. Yang, D. Ma, B. Z. Tang, Z. Zhao, Angew. Chem. Int. Ed., 2024, 63, e202405418.
12. J. Zeng, S. Song, Y. Fu, X. Peng, B. Tang, Z. Zhao, Sci. Adv., 2025,11, eadt7899.